

A TGA study of CO₂ gasification reaction of various types of coal and biomass[†]

Tahereh Jalalabadi, Chengguo Li, Hakgyu Yi and Donggeun Lee^{*}

School of Mechanical Engineering, Pusan Clean Coal Center, Pusan National University, Busan 609-735, Korea

(Manuscript Received November 19, 2015; Revised February 28, 2016; Accepted March 29, 2016)

Abstract

The CO₂ gasification kinetics of various carbonaceous samples of high- and low-rank coal and a biomass were determined under CO₂ flow with increasing temperature in a Thermogravimetric analysis (TGA) coupled with Fourier transform infrared spectroscopy (FTIR). We utilized four different types of fuels and their chars with significant differences in their physico-chemical properties that are being most widely used in Korea. As a result, fuels with larger surface area and more catalytic components in ash were preferred for increasing the intrinsic reactivity of CO₂ gasification particularly for low-rank coals and biomass, respectively. It was postulated that the catalytic effect of ash components could compensate for the lack of active sites in the biomass samples. From the practical point of view, the utilization of the low-rank coal with the porous char structure with blending the biomass is recommended for a remarkable increase of the gasification rate.

Keywords: CO₂ gasification; Coal and biomass; Volatile species; Thermogravimetric analysis; Boudouard reaction

1. Introduction

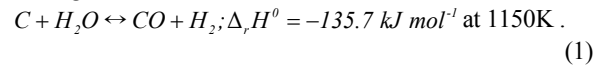
Since the industrial revolution, coal has been a major driver of human progress. As an abundant, reliable, and inexpensive natural resource, coal has been used to produce electricity by combustion and gasification [1]. The increasing rate of world energy consumption and the global warming have been the most critical issues related to world energy supplies over the decade and will be in the coming years [2].

Gasification provides an efficient way to promote coal utilization, which in contrast to combustion has a higher conversion efficiency and emits fewer air pollutants such as NO_x or SO_x owing to the low-temperature occurrence of the reaction [3]. Furthermore, gasification can be used for converting any carbonaceous materials into valuable energy products such as synthetic gas (e.g., H₂, CO, CH₄) [4, 5]. The diversity of solid fuel types such as coal, char, organic waste, and biomass constitute the main advantages of gasification [6, 7]. Recently, biomass has been widely tested as an alternative to fossil fuel for energy production because of its potential to reduce net CO₂ emission [8-11]. Biomass gasification is also one of the most promising technologies owing to its ability to convert large amounts of various types of biomass rapidly into easily storable and transportable synthetic gas or liquid [6, 7, 12].

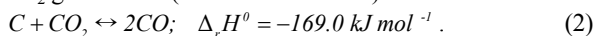
There are two types of gasification: steam gasification vs

CO₂ gasification which is often called Boudouard reaction.

Steam gasification:



CO₂ gasification (Boudouard reaction):



From Eqs. (1) and (2), one may notice that steam gasification requires less amount of energy than CO₂ gasification. In addition, since steam gasification reaction proceeds five times faster than CO₂ gasification [13], previous researches have been mainly focused on steam gasification through parametric studies such as effects of temperature, pressure, types of system devices [14-16], and types of fuel [17-19]. Nonetheless, CO₂ gasification is rather increasingly important because of its potentials: CO₂ gasification directly converts the greenhouse gas CO₂ and various solid fuels to a more useful gaseous fuel of CO; and that could be a potential route for CO₂ recycling with no need of carbon capture sequestration. More recently with the coming of a new type of coal-fueled fuel cell such as a Direct coal fuel cell (DCFC), CO₂ gasification particularly under atmospheric pressure has attracted a great deal of interest. This is because typical operation conditions of DCFC (> 700°C at 1 atm) are favorable for the CO₂ gasification; and the CO resulting from the gasification could compensate the slow electrochemical reaction of solid carbon in DCFC [20-22]. Hence many recent studies about the CO₂ gasification of vari-

^{*}Corresponding author. Tel.: +82 51 510 2365, Fax.: +82 51 512 5236

E-mail address: donglee@pusan.ac.kr

[†]Recommended by Associate Editor Taesung Kim

© KSME & Springer 2016

ous fuels were triggered as shown below.

Huo et al. [17] investigated the effect of crystallinity as well as the ash components on the gasification rate of biomass, coke, and coal chars, particularly at high temperature ($> 1000^{\circ}\text{C}$). Their results showed that the crystalline structure of fuel was an important factor affecting the gasification reactivity, whereas neither the surface area nor the content of catalytic components in ash was correlated with the reactivity. On the contrary, Duman et al. [23] reported that the gasification reactivity of various biomass fuels strongly depends on the surface area of their chars obtained during CO_2 gasification. Note that their work had been done only for the biomass with high levels of volatile substances. There are other important factors which affect the gasification reactivity, such as the types of carbon source [18, 24, 25], the use of a catalyst [26, 28], the number of active sites, and the degree of porosity [29, 30]. In addition, surface oxygenated groups and volatiles, particularly when raw fuels are considered, could make the analysis even more complex [7, 28]. Despite a large number of publications, because of the complexity and contradictions in the gasification results, the research community has not reached a solid consensus yet.

It sounds like that there exists no universal law underlying the CO_2 gasification of all the solid fuels in the world. Thus, we narrowed the research object to domestic fuels, aiming at the practical application of CO_2 gasification to power-plant industries in Korea. The first objective of this study is therefore to investigate the properties of specific solid fuels being used most widely in Korea, in connection with their gasification reactivity. Next, it should be noted that most of the gasification studies were focused on raw fuels; though the fuels come close to the char state at 700°C that the CO_2 gasification commences. When the fuels are converted into the chars, their inherent carbon structures could be exposed by removing any volatiles; thus the gasification reactivity of the chars, albeit different from that of the raw fuels, could show the intrinsic reactivity of fuels. The second objective of this study is therefore to assess the intrinsic gasification reactivity of fuels by differentiating the gasification reactivity between the raw fuels and their chars.

Here, this work utilizes four different types of fuels (a bituminous coal, two types of sub-bituminous coal, and a biomass) and their chars with substantial differences in their minerals, volatility, and surface areas. The fuels were provided from five major coal-fired power plants in Korea. While heating the four raw fuels and their prepared chars at a constant rate using a Thermo-gravimetric analyzer (TGA), mass change of each sample were monitored as a function of temperature. At the same time, emission levels of CO gas from each sample, which is a major product of CO_2 gasification reaction, were monitored by coupling Fourier transform infrared spectroscopy (FTIR) with TGA. Physico-chemical properties of the sample were also measured before and after the sample treatment and the gasification experiment, and compared with the gasification reactivity.

Table 1. Proximate and ultimate analyses of the raw samples.

Fuel	Proximate analysis (wt.%, air-dry)				Ultimate analysis (wt.%, air-dry)				
	Moi	Vol.	F.C.	Ash	C	H	O	N	S
Sub-bit (A)	17.5	38.7	38.3	5.6	58.9	5.4	14.2	0.6	1.3
Bit	3.5	30.9	48.8	16.7	69.2	4.0	6.7	1.7	0.7
Sub-bit (B)	25.9	44.5	27.3	2.1	53.4	4.8	26.9	0.6	0.2
Biomass	6.7	74.8	2.3	16.0	41.2	6.0	49.7	0.4	0.1

Table 2. Temperature-resolved variations of CO absorbance in IR spectra of evolving gases from the raw samples under the CO_2 gasification.

Fuel	N_2 adsorption (77K)		
	S_{BET} (m^2/g)	V_{total} (cm^3/g)	D_{pore} (Å)
Sub-bit (A)	3.32	0.0013	1.66
Bit	3.33	0.0054	11.49
Sub-bit (B)	0.32	0.0012	21.75
Biomass	0.14	0.0051	12.92
Sub-char (A)	217.55	0.1120	1.92
Bit-char	48.40	0.0199	30.92
Sub-char (B)	280.43	0.1333	2.71
Biomass-char	6.49	0.0094	58.42

2. Experimental approach

2.1 Sample preparation

Three coal samples, one type of high-rank (bituminous) coal named Moolarben and two low-rank (sub-bituminous) coals named Open blue and Berau from Australia, as well as a biomass sample (wood pellet) were tested in this work. All of the samples were ball-milled to a fixed size of $\sim 70 \mu\text{m}$. Chars were prepared by removing the volatile species from the raw fuel samples: 50 mg of each sample was heated with a TGA (SDT-Q600, TA Instruments) from 25°C to 900°C with a rate of $10^{\circ}\text{C}/\text{min}$ under Ar gas flow with a rate of 100 ml/min.

The results of proximate and ultimate analyses of the raw samples are presented in Table 1. The proximate analysis was conducted using the TGA following the process of American Society for Testing and Materials Standard (ASTM E1131). The ultimate analysis was performed using a vario MICRO cube which was subjected to a temperature of 1150°C with sulfanilic acid used as a standard solution. In this work, the fuel samples were named after the types of fuels: Berau as Sub-bit (A), Open blue as Sub-bit (B), Moolarben as Bit and a wood pellet as Biomass.

2.2 Sample characterization

The thermal behavior and reactivity of the raw fuel and char samples were studied by measuring the mass change of the samples with a TGA (Q-50, TA Instruments, USA) while flowing either an inert gas (Ar: 100 ml/min) or carbon dioxide

Table 3. Ash constituent analysis (wt%) of the raw samples.

	SiO ₂	Al ₂ O ₃	Fe ₂ O ₃	CaO	MgO	Na ₂ O	K ₂ O	TiO ₂	SO ₃	A.I.
Sub-bit (A)	37.04	12.13	8.52	6.81	2.54	6.47	1.08	1.24	7.89	2.797
Bit	72.47	12.25	0.66	0.02	0.14	0.08	0.32	0.79	0.12	0.268
Sub-bit (B)	37.17	27.27	8.44	8.12	2.77	0.32	0.48	1.85	13.0	0.677
Biomass	17.22	5.52	6.27	32.89	13.90	3.57	10.46	0.92	4.01	47.20

(CO₂: 100 ml/min). Coupling the TGA with the FTIR (Nicolet 380), we monitored continually FTIR peak intensity of CO gas with increasing the TGA temperature. As the CO gas results not only from the CO₂ gasification but also from the decomposition of surface oxygenated groups or volatiles of fuels [4, 5, 28, 31], the intrinsic emission levels of CO by the CO₂ gasification was identified by comparing the CO levels emitting from the raw fuels and their chars. Amounts of approximately 10 mg of samples were tested with a dynamic thermogravimetric method in a range of 25 to 900°C at a heating rate of 10°C/min. To confirm the results, each of the tests was repeated three times.

Surface area and pore volume of the samples were obtained using nitrogen gas adsorption experiment at 77 K and applying the Brunauer-Emmett-Teller (BET) equation (ASAP 2020; Micromeritics Co., USA). The pore diameters (D_{pore}) of the samples were acquired using the Barrett-Joyner-Halenda (BJH) method [31-33]. Table 2 summarizes the results and shows that the chars generally have a larger surface area after removal of the volatile species, and thus provide a greater active area for CO₂ molecules in the gasification procedure.

The ash components of the raw fuel samples were analyzed using a X-Ray fluorescence spectroscopy (XRF-1700; Shimadzu, Japan) for the chars and the results are listed in Table 3. Among all samples, the bituminous coal denotes the highest content of SiO₂ and Al₂O₃ which are known as inert species while the biomass shows the lowest levels. As for the alkaline metals which play a role of catalysts, on the contrary, the biomass has noticeably high levels of the catalytic species in contrast to the bituminous coal. The Sub-bits (A) and (B) have intermediate levels of inert species and catalytic species in ash.

3. Results and discussion

Fig. 1(a) illustrates the dynamic TGA profiles of the relative mass for the present four samples (Sub-bit (A), Sub-bit (B), Bit and Biomass) in an Ar flow. The relative mass in units of % was defined based on the sample mass at 100°C above which water contribution is believed negligible. With the Ar flow, devolatilization accompanied by pyrolysis to some extent normally takes place over the raw sample, leading to a release of gases such as CO, H₂, CH₄, and CO₂ [4, 5] and the resultant mass loss. Thus, the mass loss occurring at this char-making process in Ar flow might be attributed to the volatile contribution. As summarized in Table 4, a comparison of the mass loss of the samples in Fig. 1(a) indicates that among the samples, the bituminous coal (Bit) has the lowest level of

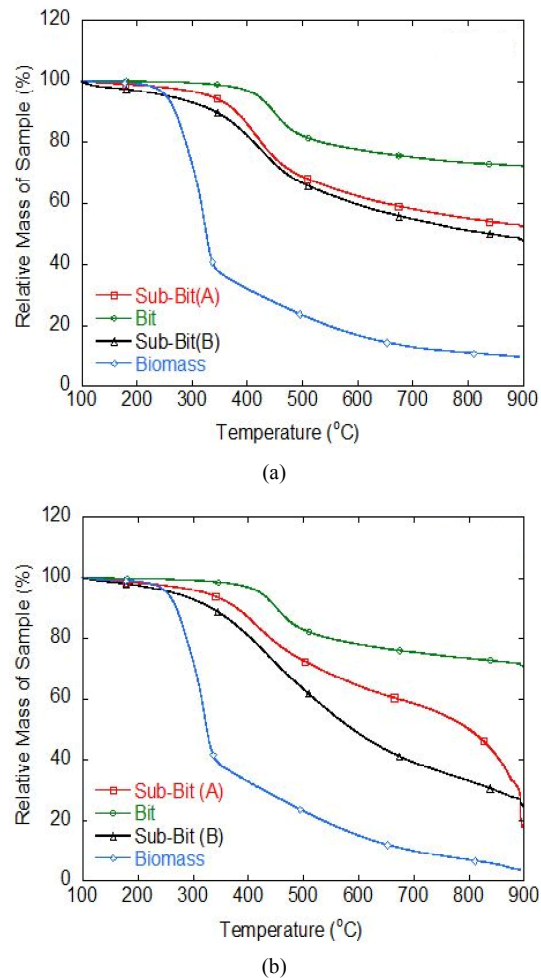


Fig. 1. Dynamic TGA profiles of relative mass of the raw samples in (a) Ar; (b) CO₂ flow.

volatiles, with a mass loss of 28%. In contrast, the Sub-bit (A) and (B) samples are both more volatile with mass losses of nearly 41 and 52%, respectively. The Biomass shows that 87% of the sample is volatile. These results are reasonably consistent with the results of the proximate analysis shown in Table 1.

Moreover, drastic mass losses in all of the fuel samples occur mostly below 700°C (specifically from 250°C to 600°C). Above 700°C, the mass only slightly decreases for all samples: Bit, 2.5%; Sub-bit (A), 5%; Sub-bit (B), 7%; Biomass, 2.6%. These small mass losses imply that nearly all of the volatile species left the solid surface while the rest of the fuel

Table 4. Mass loss percentages of the raw samples during the devolatilization and CO₂ gasification processes.

	Mass loss ^a in Ar flow	Mass loss ^a in CO ₂ flow	Mass loss ^b in CO ₂ flow from 700°C to 900°C
Sub-bit (A)	41.2%	82.2%	40.5%
Bit	28.0%	29.5%	3.5%
Sub-bit (B)	52.2%	75.8%	15.0%
Biomass	87.3%	96.6%	9.0%

^aDecrease of relative mass of samples observed when heating from 100°C to 900°C;

^bDecrease of relative mass of samples observed in the temperature range.

got close to a char, named semi-char with such low levels of remaining volatiles. Thus, it is assumed that during the creation of the char, most of the devolatilization occurs before reaching the CO₂ gasification reaction temperature (700°C).

Fig. 1(b) shows the profiles of the relative mass of the same raw samples in CO₂ flow. The observed results display similar TGA curves to those in Ar flow (Fig. 1(a)) below 700°C, suggesting that the CO₂ gas is inert in the temperature range. As temperature increases from 700 to 900°C, the mass losses of the Sub-bit (A) and (B), and the Biomass sample were 40.5, 15.0, and 8.9%, respectively (refer to the third column of Table 4). The high-temperature mass losses are obviously higher than those in Ar flow (Fig. 1(a)), suggesting the possible occurrence of the CO₂ gasification. On the other hand, the overall mass loss of the Bit sample in CO₂ flow is similar to that of the sample in Ar flow, with only a 1.5% difference, indicating that the Bit sample is the least reactive to CO₂.

To understand what caused the difference in the high-temperature mass losses, we compared the specific surface areas of the char samples rather than their pristine fuel samples, because the raw fuels get close to their chars in nature above 700°C. From Table 2, the char of the Bit sample (named Bit-char) had a smaller surface area (see Table 2) in comparison to the Sub-char samples, which seems to explain the lowest reactivity of the Bit sample. However, it should be noted that the order of surface areas of the chars is not always the same as the order of reactivity. For example, the Biomass sample with the least porous char did not show the lowest reactivity; its high-temperature mass loss associated with the CO₂ gasification was indeed the second lowest. This implies that there is another factor improving its reactivity such as catalytic agents, which might relate to the ash composition in Table 3 (will be explained later).

Fig. 2 shows the variations of CO peak intensity in FTIR spectra for the raw samples, which were obtained with an increment of 25°C during the CO₂ gasification process. For the Sub-bit (A) and (B) samples, CO is generated even below 700°C presumably due to devolatilization, followed by a sharp increase in the CO absorbance above 700°C. The sharp increase of the two sub-bituminous coals signifies a relative dominance of the CO₂ gasification reaction at high tempera-

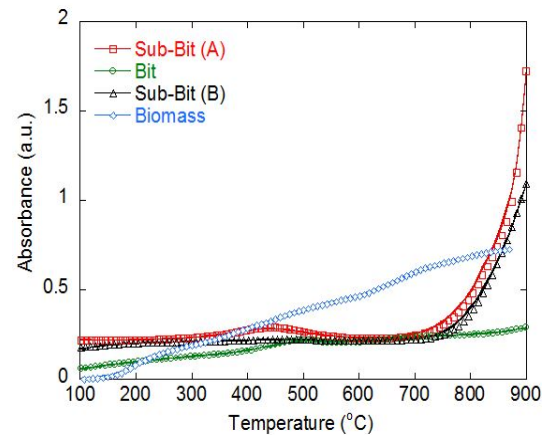


Fig. 2. Temperature-resolved variations of CO absorbance in IR spectra of evolving gases from the raw samples under the CO₂ gasification.

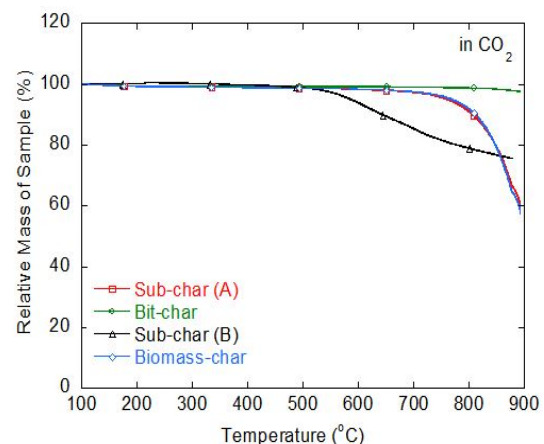


Fig. 3. Dynamic TGA profiles of relative mass of the first prepared char samples under CO₂ gasification.

tures. The highest absorbance belongs to the Sub-bit (A) sample which showed the largest mass loss above 700°C in Fig. 1(b). On the contrary, the Biomass and Bit samples show a gradual increase in the IR absorbance with increasing the temperature. No such sharp increase in the CO absorbance represents either relative dominance of the devolatilization (perhaps corresponding to the Biomass sample with the highest level of volatiles) or insignificant CO₂ gasification reaction of the samples (corresponding to the Bit sample). As for the case of Biomass releasing massive amounts of volatiles, such product gases evolving from the sample could hinder the diffusive contact of the incoming CO₂ gas with the Biomass in the sample pan of TGA and then reduce the CO₂ gasification rate [34]. In any case, ruling out the contribution of the devolatilization to the mass loss is very likely required for better understanding the material dependency of the CO₂ gasification reaction. For this purpose, we repeated the same TGA experiment (for CO₂ gasification in Fig. 1(a)) for the chars (prepared from the first run of the TGA with Ar flow).

Fig. 3 presents the TGA profiles of the relative mass of the

char samples with CO_2 flow. In the figure, Sub-char (A) and (B) represent the chars originated from the Sub-bit (A) and (B) samples, respectively, and the Bit-char and Biomass-char are named likewise. After removal of volatiles, the mass of the Sub-char (A), Bit-char, and Biomass-char, as expected, begin to decrease above 700°C in CO_2 mainly due to the CO_2 gasification. The Bit-char and Sub-char (A) denote mass losses of 2.0% and 40.5%, respectively, which are similar to the high-temperature mass losses that their raw fuel samples underwent from 700°C to 900°C (refer to Table 4). The Biomass-char sample exhibits the same mass loss behavior as the Sub-char (A), reaching the maximum mass loss of $\sim 40\%$ in contrast to 9% that its raw sample showed. The difference in the mass loss is caused by difference in the reference sample mass for calculation of the relative mass: initial mass of the char sample versus the mass of the raw sample at 100°C . Besides, there still remains another unresolved mystery: why only the mass of Sub-char (B) begins to decrease at 550°C in CO_2 , far below 700°C ? To check whether the low-temperature mass loss is associated with an abnormal CO_2 gasification reaction or not, we inspected the quality of the prepared chars by repeating the char-making process once more.

In Fig. 4, the Sub-char (B) still shows a mass loss of nearly 10% during the second char-making process with Arflow, which is almost three times higher than those of the other chars. This suggests that the first run of the char-making process is not necessarily efficient for removal of volatiles, leaving behind some of volatile matters in the resultant chars. It is of particular interest to note that the Sub-char (B) in Table 2 is the most porous, so that it might be able to hold the volatile matters inside pores longer. If this is the case, the low-temperature mass loss of the Sub-char (B) in CO_2 flow observed in Fig. 3 should disappear after complete removal of the remaining volatiles via the second run of the char-making process in Fig. 4(a). Hence, the CO_2 gasification experiment has been carried out again for the char samples that have been such treated.

As shown with all of the double-treated char samples in Fig. 4(b), there is no notable evidence about the abnormal CO_2 gasification below 700°C , and most of the mass loss occurs above 700°C . The mass loss of the Sub-char (B) was found to be 38.9%, very close to those of the Sub-char (A) and Biomass-char samples, but order of magnitude larger than that of the Bit-char sample (1.7%). Let us recall Table 2 in which the Sub-chars (A) and (B) have much large BET surface areas as compared to the Bit-char. Thus, it is naturally conjectured that the surface area or porosity of the char samples plays a key role in determining the apparent reactivity of CO_2 gasification reaction, at least in the three samples. This result is compatible with other claims that char with a larger BET surface area has higher gasification reactivity [15].

Let us return the remaining final question about the abnormally high reactivity of the non-porous Biomass-char. Since any contributions of volatiles are completely removed, it seems to be associated with ash residing the chars. Huang et al.

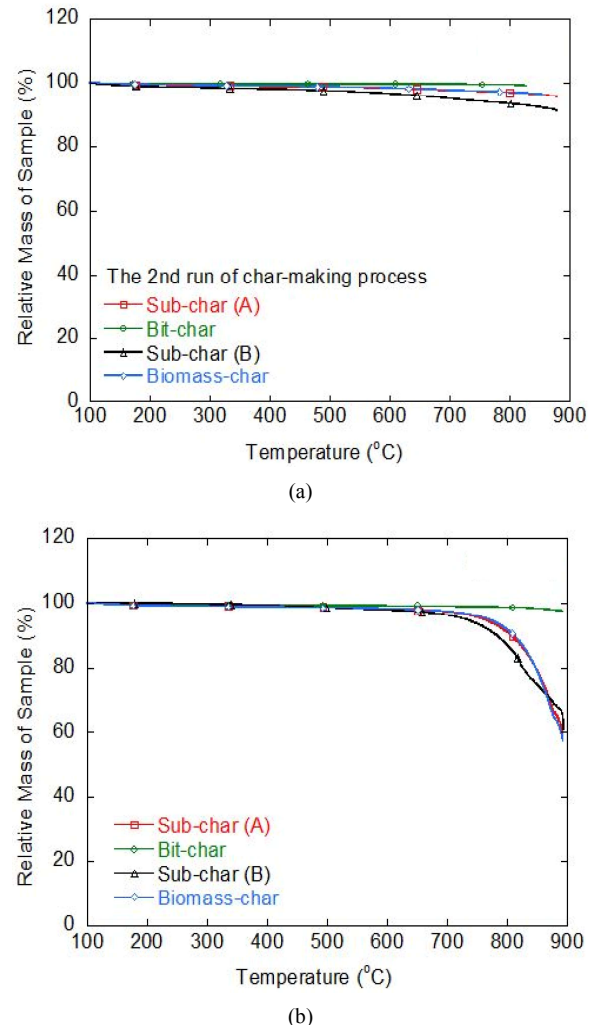


Fig. 4. Dynamic TGA profiles of relative mass of (a) the first prepared char samples during their second char-making process with Ar flow; (b) the second prepared char samples under CO_2 gasification.

[26, 35, 36] reported the effects of the chemical constituents of ashes on the kinetics of the CO_2 gasification reaction. Some species, such as silica and alumina, play a hindering role, in contrast to the catalytic role of alkaline metals ($\text{K} > \text{Na} > \text{Ca} > \text{Fe} > \text{Mg}$) in the CO_2 gasification reaction. Hence, an alkaline index (A.I.) representing the content of catalytic species (like alkaline metals) relative to the deactivating species was defined as follows [7, 35, 37] and used for assessing the catalytic activity of ashes in the chars.

$$\text{Alkaline index} = \text{ash content (wt\%)} * \{(\text{Fe}_2\text{O}_3 + \text{CaO} + \text{MgO} + \text{Na}_2\text{O} + \text{K}_2\text{O}) / (\text{SiO}_2 + \text{Al}_2\text{O}_3)\} \quad (3)$$

The XRF data in Table 3 provide comprehensive information about the ash compositions of the four samples in this study. Major non-catalytic species such as silica and alumina are distributed in a vast range from 22% in the Biomass to 84% in the Bit sample, while catalytic elements such as CaO

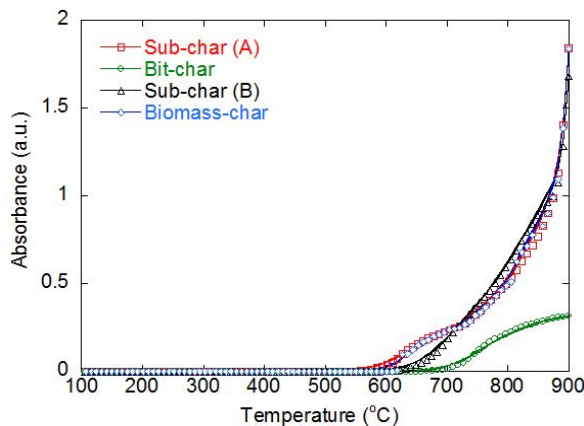


Fig. 5. CO absorbance in IR spectra of evolving gases from the char samples under the CO_2 gasification.

vary from almost zero (the Bit sample) to 33% (the Biomass). Note that the Biomass has an order of magnitude larger A.I. value than the rest of fuels, together with the largest amount of ash. This might explain why the non-porous Biomass has a comparable CO_2 gasification reactivity to the much more porous sub-bituminous samples. Thus we believe that the effect of ash mineral content prevails at least with regard to the reactivity of the Biomass sample. It is also interesting to note that the Sub-bit (B), that is more porous than the Sub-bit (A), has a smaller A.I. value. Such conflict between the surface area and A.I. might lead to the similar gasification reactivity of the two sub-bituminous samples.

To confirm the properties of the mass loss curves in the char samples, the IR absorbance of CO gas evolving from the mass-loss experiment was measured by FTIR and shown in Fig. 5. Overall trend in the curves looks similar to that in Fig. 4(b). The samples of Sub-char (A) and (B) as well as the Biomass show an identical rise in the CO absorbance, while the Bit-char sample is the least reactive.

4. Conclusion

An investigation of various types of coal and a biomass sample under the CO_2 gasification process was done in an effort to understand the effect of the physio-chemical properties of these samples on the reaction rate. The comparison of the devolatilization and the gasification properties of the raw fuel samples yielded that large amount of devolatilized gases, e.g., from Sub-bit (B) and Biomass samples, overwhelmed the mass loss, which might mislead TGA users to underestimate their CO_2 gasification reactivity and misjudge an abnormal CO_2 gasification reaction below 700°C. In particular, repeating the char-making process twice, when a dynamic TGA mode was used, was at least required for complete removal of volatiles for the Sub-bit (B) sample. As a result of the char samples, fuels with larger surface area and more catalytic components in ash denoted higher reactivity of CO_2 gasification. In this aspect, the Bit sample, that has the lowest surface

area and no catalytic species with the lowest alkaline index, was almost nonreactive to CO_2 in the present condition. From the practical point of view, it is recommended that the utilization of the low-rank coal with the porous char structure with blending the biomass gives rise to a remarkable increase of the gasification rate.

Acknowledgment

This work was supported by grants from the Human Resources Development program (No. 20144010200780) of the Korea Institute of Energy Technology Evaluation and Planning (KETEP) funded by the Korean government's Ministry of Trade, Industry and Energy, and by the MSIP and National Research Foundation (NRF) of Korea (2014M3C8A5030614). It was also supported by the Global Frontier R&D Program of the Center for Multiscale Energy Systems, funded by the National Research Foundation under the Ministry of Education, Science and Technology, Korea (No. 2012M3A6A7054863).

References

- [1] D. Erincin, A. Sinag, Z. Misirloglu and M. Canel, Characterization of burning and CO_2 gasification of chars from mixtures of Zonguldak (Turkey) and Australian bituminous coals Original, *Ener. Convers. Manage.*, 46 (2005) 2748-2761.
- [2] P. Lahijani, Z. A. Zainal, M. Mohammadi and A. R. Mohamed, Conversion of the greenhouse gas CO_2 to the fuel gas CO via the Boudouard reaction: A review, *Renew. Sust. Energ. Rev.*, 41 (2015) 615-632.
- [3] L. Guo and H. Jin, Boiling coal in water: Hydrogen production and power generation system with zero net CO_2 emission based on coal and supercritical water gasification, *Int. J. Hydrogen Energ.*, 38 (2013) 12953-12967.
- [4] S. Singh, C. Wu and P. Williams, Pyrolysis of waste materials using TGA-MS and TGA-FTIR as complementary characterisation techniques, *J. Anal. Appl. Pyrol.*, 94 (2012) 99-107.
- [5] Y. Wang and D. A. Bell, Reaction kinetics of Powder River Basin coal gasification in carbon dioxide using a modified drop tube reactor, *Fuel*, 140 (2015) 616-625.
- [6] J. Matsunami, S. Yoshida, Y. Oku, O. Yokota, Y. Tamura and M. Kitamura, Coal gasification by CO_2 gas bubbling in molten salt for solar/fossil energy hybridization, *Solar Energy*, 68 (2000) 257-261.
- [7] P. Lahijani, Z. A. Zainal, M. Mohammadi and A. R. Mohamed, Conversion of the greenhouse gas CO_2 to the fuel gas CO via the Boudouard reaction: A review, *Renew. Sust. Energ. Rev.*, 41 (2015) 615-632.
- [8] R. Zanzi, K. Sjostrom and E. Bjornbom, Rapid high-temperature pyrolysis of biomass in a free-fall reactor, *Fuel*, 75 (1996) 545-550.
- [9] V. Stanislav, G. Christina and S. Vassil, Advantages and disadvantages of composition and properties of biomass in

comparison with coal: An overview, *Fuel*, 158 (2015) 330-350.

[10] S. Vassilev, D. Baxter, L. Anderson and C. Vassileva, An overview of the chemical composition of biomass, *Fuel*, 89 (2010) 913-933.

[11] S. Vassilev, C. Vassileva and D. Baxter, Trace element concentrations and associations in some biomass ashes, *Fuel*, 129 (2014) 292-313.

[12] J. Fermoso, M. V. Gil, C. Pevida, J. J. Pis and F. Ruberia, Kinetic models comparison for non-isothermal steam gasification of coal-biomass blend chars, *Chem. Eng. J.*, 161 (2010) 276-284.

[13] F. Mermoud, S. Salvador, L. Van de Steene and F. Golfier, Influence of the pyrolysis heating rate on the steam gasification rate of large wood char particles, *Fuel*, 85 (2006) 1473-1482.

[14] F. Min, M. Zhang, Y. Zhang, Y. Cao and W.-P. Pan, An experimental investigation into the gasification reactivity and structure of agricultural waste chars, *J. Anal. Appl. Pyrol.*, 92 (2011) 250-257.

[15] M. Malekshahian and J. M. Hill, Kinetic analysis of CO₂ gasification of petroleum coke at high pressures, *Energy Fuels*, 25 (2011) 4043-4048.

[16] L. Ren, J. Yang, F. Gao and J. Yan, Laboratory Study on Gasification Reactivity of Coals and Petcoke in CO₂/Steam at High Temperatures, *Energy Fuels*, 27 (2013) 5054-5068.

[17] W. Huo, Z. Zhou, X. Chen, Z. Dai and G. Yu, Study on CO₂ gasification reactivity and physical characteristics of biomass, petroleum coke and coal chars, *Bioresour. Technol.*, 159 (2014) 143-149.

[18] R. Habii, J. Kopyscinski, M. Masnadi, S. J. Lan, J. Grace, C. Mim and J. Hill, Co-gasification of biomass and non-biomass feedstocks: Synergistic and inhibition effects of switchgrass mixed with sub-bituminous coal and fluid coke during CO₂ gasification, *Energy Fuels*, 27 (2013) 494-500.

[19] P. Wang, S. W. Hedges, K. Casleton and C. Guenther, Thermal behavior of coal and biomass blends in inert and oxidizing gaseous environments, *Int. J. Clean Coal and Energ.*, 1 (2012) 35-42.

[20] C. Li, H. Yi and D. Lee, On-demand supply of slurry fuels to a porous anode of a direct carbon fuel cell: attempt to increase fuel-anode contact and realize long-term operation, *J. Power Sources*, 309 (2016) 99-107.

[21] C. Li, E. K. Lee, Y. T. Kim and D. Lee, Enhancing triple-phase boundary at fuel electrode of direct carbon fuel cell using a fuel-filled ceria-coated porous anode, *Int. J. Hydrogen Energy*, 39 (2014) 17314-17321.

[22] C. Li, H. Yi, T. Jalalabadi and D. Lee, Thermal decomposition of alkane hydrocarbons inside a porous Ni anode for fuel supply of direct carbon fuel cell: Effects of morphology and crystallinity of carbon, *J. Power Sources*, 294 (2015) 284-291.

[23] G. Duman, M. A. Uddin and J. Ynik, The effect of char properties on gasification reactivity, *Fuel Process. Technol.*, 118 (2014) 75-81.

[24] S. Idris, N.A. Rahman, K. Ismail, A. B. Alias, Z. A. Rashid and M. J. Aris, Investigation on thermochemical behaviour of low rank Malaysian coal, oil palm biomass and their blends during pyrolysis via thermogravimetric analysis (TGA), *Bioresour. Technol.*, 101 (2010) 4584-4592.

[25] C. D. Blasi, Combustion and gasification rates of lignocellulosic chars, *Prog. Energy and Combust. Sci.*, 35 (2009) 121-140.

[26] Y. Huang, X. Yin, C. Wu, C. Wang, J. Xie and Z. Zhou, Effects of metal catalysts on CO₂ gasification reactivity of biomass char, *Biotechnol. Adv.*, 27 (2009) 568-572.

[27] J. Kopyscinski, R. Habii, C. A. Mims and J. Hill, K₂CO₃-catalyzed CO₂ gasification of ash-free coal: Kinetic study, *Energy Fuels*, 27 (2013) 4875-4883.

[28] Y. H. Kim, Y. T. Kim, S. H. Kim and D. Lee, Catalytic oxidation kinetics of iron-containing carbon particles generated by spraying ferrocene-mixed with diesel fuel into a hydrogen-air diffusion flame, *Carbon*, 48 (2010) 2072-2084.

[29] Y. T. Kim, D. K. Seo and J. Hwang, Study of the effect of coal type and particle size on char-CO₂ gasification via gas analysis, *Energy Fuels*, 25 (2011) 5044-5054.

[30] K. Xu, S. Hu, S. Su, C. Xu, L. Sun, C. Shuai, L. Jiang and J. Xiang, Study on char surface active sites and their relationship to gasification reactivity, *Energy Fuels*, 27 (2012) 118-125.

[31] S. Eom, S. Ahn, Y. Rhie, K. Kang, Y. Sung, C. Moon, G. Choi and D. Kim, Influence of devolatilized gases composition from raw coal fuel in the lab scale DCFC (direct carbon fuel cell) system, *Energy*, 74 (2014) 734-740.

[32] S. Ahn, S. Eom, Y. Rhie, Y. Sung, C. Moon, G. Choi and D. Kim, Application of refuse fuels in a direct carbon fuel cell system, *Energy*, 51 (2013) 447-456.

[33] S. Ahn, S. Eom, Y. Rhie, Y. Sung, C. Moon, G. Choi and D. Kim, Utilization of wood biomass char in a direct carbon fuel cell (DCFC) system, *Appl. Energy*, 105 (2013) 207-216.

[34] K. Matsuoka, S. Hosokai, Y. Kaoto, K. Kuramato, Y. Suzuki, K. Norinaga and J. Hayashi, Promoting gas production by controlling the interaction of volatiles with char during coal gasification in a circulating fluidized bed gasification reactor, *Fuel Processing Technol.*, 16 (2013) 308-316.

[35] L. Zhang, J. Huang, Y. Fang and Y. Wang, Gasification reactivity and kinetics of typical Chinese anthracite chars with steam and CO₂, *Energy Fuel*, 20 (2006) 1201-1210.

[36] Y. Huang, X. Yin, C. Wu, C. Wang, J. Xie, Z. Zhou, L. Ma and H. Li, Effects of metal catalysts on CO₂ gasification reactivity of biomass char, *Biotechnol. Adv.*, 27 (2009) 568-572.

[37] M. Sakawa, Y. Sakurai and Y. Hara, Influence of coal characteristics on CO₂ gasification, *Fuel*, 61 (1982) 717-720.



Donggeun Lee is a professor at School of Mechanical Engineering, Pusan National University and is now leading a nanoparticle engineering lab. More information is available in <http://home.pusan.ac.kr/~mnht>.